IEEE Access
Multidisciplinary | Rapid Review | Open Access Journal

Received June 18, 2021, accepted June 29, 2021, date of publication July 6, 2021, date of current version July 19, 2021.

Digital Object Identifier 10.1109/ACCESS.2021.3095057

Enhanced 2-DOF PID Controller Tuning Based on an Uncertainty and Disturbance Estimator With Experimental Validation

VICENTE BALAGUER[1], ANTONIO GONZÁLEZ[2], PEDRO GARCÍA[1], AND FRANCISCO BLANES[1]

[1]Instituto de Automática e Informática Industrial, Universitat Politècnica de València, 46022 Valencia, Spain
[2]Departamento de Ingeniería de Sistemas y Automática, Universitat Politècnica de València, 46022 Valencia, Spain

Corresponding author: Antonio González (angonsor@upv.es)

This work was supported by projects FPI-UPV PAID-01-17, Universitat Politècnica de València (Spain), and TIN2017-86520-C3-1-R, Ministerio de Economía y Competitividad (Spain).

ABSTRACT In this paper a novel tuning procedure for Two-Degree-of-Freedom (2-DOF) PID controllers is proposed. The tuning methodology is based on an Uncertainty and Disturbance Estimator. As a result, an equivalent 2-DOF PID controller with simpler tuning rules is obtained. One advantage of the proposed method is that tracking performance and disturbance rejection can be accommodated separately in control synthesis. Moreover, the trade-off between disturbance rejection and robustness can easily be adjusted by tuning a single parameter without affecting the desired set-point tracking specifications. Numerical comparisons with well-known tuning methods are performed to illustrate the advantages of the proposed method. Finally, the effectiveness of the proposal is experimentally validated in an open-loop unstable plant consisting of a test-bed quadrotor platform.

INDEX TERMS PID controller, unstable systems, time-delay, disturbance observers, linear matrix inequality.

I. INTRODUCTION

Proportional-Integrative-Derivative (PID) control is still one of the most widely used in many industrial processes owing to its simplicity and robustness [1]–[3]. The key advantage is that a PID controller can easily be tuned without any in-depth knowledge of control [4] by intutively designing the PID control components: the Integrative part contributes to eliminate steady-state errors, but has a negative impact in the transient behavior; the Derivative part can achieve a faster response, but leads to a worse disturbance rejection; and the Proportional gain can be helpful to adjust the compromise between both aspects to some extent. One of the most well-known methods for PID tuning is the classic Ziegler-Nichols rules [5], which has the advantage of providing specific tuning rules for a wide variety of plants in order to meet reasonable requirements. Ziegler-Nichols method offers a very good disturbance response for integrating processes, but generally exhibits poor performance for processes with dominant time delay and rather aggressive control actions [6]. Apart from the Ziegler-Nichols method, many efforts have concentrated on finding improved PID control synthesis methods. Some of them are related to classic control design approaches such as the frequency-domain [7] or root locus method [8] and other extensions for nonlinear plants [9], while other more sophisticated methods for PID control design aimed at improving performance are available under fractional order PID [10]–[12], or PID with time predictors [13]. Other related works have addressed the PID control synthesis by means of complex numerical optimizations [14], [15].

Nevertheless, for many control engineering applications, disturbance rejection performance can be more relevant than set-point tracking [16]. Hence, controller synthesis has recently taken into consideration disturbance rejection, rather than set-point tracking. For instance, by means of One-Degree-of-Freedom (1-DOF) PID structure, set-point tracking performance and disturbance rejection requirements cannot generally be simultaneously achieved for control applications [17]. In order to circumvent this drawback, a Two-Degree-of-Freedom (2-DOF) PID was presented

The associate editor coordinating the review of this manuscript and approving it for publication was Guillermo Valencia-Palomo.

in [18], [19] so as the set-point tracking and the disturbance rejection can be handled by tuning a PID controller for each control loop. For control design, analytical [20]–[23] and numerical methods [24] were considered in order to handle both specifications. Other popular control design approaches such as the AMIGO method [25], the internal model control (IMC) [26], [27] and the SIMC method [28] offer a simple guide for tuning the PID control parameters. Nevertheless, such methods might lead to poor performance when they are applied to integrating, unstable and non-minimum phase processes if the tuning is not properly addressed [29]. Moreover, precise knowledge of the system model is often required to tune the controller adequately [30], [31].

The actual controlled system is inevitably affected by model uncertainties and external disturbances, which might lead the closed-loop system to instability if they are not considered in control synthesis. In contrast to PID techniques, which are error-based, Disturbance Observer Based Control (DOBC) has been developed from a model-based perspective. DOBC is designed to cope with model uncertainties and external disturbances [32]. The underlying idea behind DOBC is that, given a theoretical model of the plant and its input/output measurements, an equivalent disturbance that 'explains' the unknown behavior is obtained and then used to counteract its effects. Hence DOBC techniques are focused on making the plant to behave like the theoretical one. The disturbance observer approach has been successfully applied to a wide range of applications, such as robotic manipulators [33], high speed XY positioning [34], missile control [35], and quadrotors [36], [37], among others. Due to its potential applications, the DOBC approach has been widely studied over the past years. Generalized Extended State Observer (GESO) [38], Disturbance Observer (DOB) [39], [40], Active Disturbance Rejection Control (ADRC) [41], and Uncertainty and Disturbance Observer (UDE) [42] are some examples of DOBC techniques.

In this paper, an equivalent 2-DOF PID from an UDE control scheme is presented for first and second order systems with time delays, including unstable systems. The proposed method can be extended to higher-order systems by reducing them to a lower-order, and further treating the unknown behavior as a disturbance. This approach, initially raised in [43], makes it possible to obtain a 2-DOF PID easily with only the set-point requirement and a single-parameter to deal with the compromise between disturbance rejection performance and robustness. It is worthwhile mentioning that the addition of a lead-lag filter allows to deal with more advanced systems than the previous proposal. The closed-loop robust stability analysis with guaranteed disturbance rejection in the sense of H_∞ norm for systems with time-varying parametric uncertainties is formulated in terms of Linear Matrix Inequalities (LMIs) [44]. In addition, some representative examples are studied and an experimental validation is validated in a test-bed quadrotor platform.

The rest of the paper is organized as follows: the problem statement is given in Section II. The proposed 2-DOF PID control scheme with the lead-lag filter is presented in Section III. In Section IV, the trade-off between closed-loop disturbance rejection and robustness against model uncertainties is discussed. Comparative simulation results are provided in Section V. Experimental results with a quadrotor test-bed platform are performed in Section VI, and finally, some conclusions and perspectives are gathered in Section VII.

II. PROBLEM STATEMENT

Consider the following SISO system expressed in Laplace domain subject to a matched disturbance:

$$Y(s) = G(s)e^{-Ls}\left(U(s) + D(s)\right) \tag{1}$$

where $G(s) = \frac{b_{n-1}s^{n-1}+\cdots+b_0}{s^n+a_{n-1}s^{n-1}+\cdots+a_0}$ is the transfer function of the plant system, $L \geq 0$ is a positive delay, $U(s)$ (or $u(t)$ in time-domain) is the control input, and $D(s)$ represents a disturbance signal.

Note that $G(s)$ can be represented in the state-space canonical form as:

$$\begin{aligned} A &= \begin{bmatrix} 0 & & I_{n-1} & \\ -a_0 & -a_1 & \cdots & -a_n \end{bmatrix}, \quad B = \begin{bmatrix} 0 \\ b_0 \end{bmatrix}, \\ C &= \begin{bmatrix} 1 & b_1/b_0 & \cdots & b_{n-1}/b_0 \end{bmatrix} \end{aligned} \tag{2}$$

The goal is to regulate the state $x(t)$ of the closed-loop system through $u(t)$ so that it asymptotically tracks the state of a reference model with the desired stable closed-loop dynamics given by

$$\dot{x}_m(t) = A_m x_m(t) + B_m r(t), \tag{3}$$

where $r(t) \in \mathcal{R}$ is the desired reference signal, and

$$\begin{aligned} A_m &= \begin{bmatrix} 0 & & I_{n-1} & \\ -a_{0m} & -a_{1m} & \cdots & -a_{nm} \end{bmatrix}, \\ B_m &= \begin{bmatrix} 0 \\ a_{0m} \end{bmatrix}, \quad C_m = C \end{aligned} \tag{4}$$

being A_m a Hurwitz matrix.

Hence, the objective is to find a simple criterion to design the controller parameters $u(t)$ with a 2-DOF PID control scheme so that the closed-loop dynamics (given by the choice of the coefficients $a_{im},\ i = 0, 1, \ldots, n$ in (3)) and disturbance rejection performance (given by a single scalar tuning parameter, introduced later) can be designed separately.

III. PROPOSED CONTROL SYNTHESIS METHOD

In this section the proposed 2-DOF PID control scheme is developed. First, a general view of the UDE is provided, showing its inherent 2-DOF structure. Finally, the equivalence between the obtained control and the 2-DOF PID with lead-lag cascade filter is settled for the most representative plant models.

A. PRELIMINARIES

Let us define the tracking error of the system state as

$$e(t) = x_m(t) - x(t), \tag{5}$$

Differentiating (5), and taking into account (1) and (3), the following expression is obtained

$$\dot{e}(t)=A_m e(t)+B_m r(t)+(A_m-A)x(t)-Bu(t)-Bd(t). \quad (6)$$

or equivalently in the Laplace domain:

$$\dot{E}(s)=A_m E(s)+B_m R(s) +(A_m-A)X(s)-BU(s)-BD(s).$$

Let $B^+=(B^TB)^{-1}B^T$ the pseudo-inverse matrix of B, satisfying $B^+B=1$ and $B^+=\begin{bmatrix}0_{n-1} & 0\\ 0 & 1\end{bmatrix}$. From the definition of matrices A, A_m, B, B_m in (2), (4), and the fact that A_m is Hurwitz, it is easy to see that the tracking error $e(t)$ in (6) will be asymptotically stable taking into account the closed-loop response given by the eigenvalues of A_m by defining $U(s)$ as:

$$U(s)=B^+[(A_m-A)X(s)+B_m R(s)]-D(s), \quad (7)$$

Note that $U(s)$ cannot be implemented since $D(s)$ is unknown and unmeasurable. Nevertheless, from the system model, the disturbance $D(s)$ can be approximated in the frequency domain by using a strictly proper low-pass filter $Q(s)$ with unity gain:

$$\hat{D}(s)=Q(s)B^+[(sI_n-A)X(s)-BU(s)], \quad (8)$$

where $Q(s)=1/(Ts+1)$ is the filter and T is the parameter which makes it possible to tune the filter bandwidth. This single scalar parameter will be the key to adjusting the trade-off between robustness and disturbance rejection without impacting the closed-loop dynamics (as later discussed). Consequently, an implementable control scheme is derived from (7) as:

$$U(s)=B^+[(A_m-A)X(s)+B_m R(s)]-\hat{D}(s), \quad (9)$$

By substituting (8) into (9) we obtain:

$$U(s)=\frac{1}{1-Q(s)}B^+\Big((A_m-A)X(s) -Q(s)(sI_n-A)X(s)+B_m R(s)\Big). \quad (10)$$

It can be deduced from the state-space representation given in (2) that $Y(s)=b_0X_1(s)+b_1sX_2(s)+\cdots+b_{n-1}s^{n-1}X_n(s)$. Therefore, the following equivalence holds:

$$X(s)=\frac{b_0\mathcal{W}_{n-1}(s)}{b_{n-1}s^{n-1}+\cdots+b_0}Y(s) \quad (11)$$

where $\mathcal{W}_{n-1}(s)=\begin{bmatrix}1 & s & s^2 & \cdots & s^{n-1}\end{bmatrix}^T$. By replacing $X(s)$ into (10) and rearranging terms, the control action $U(s)$ can be expressed as

$$U(s)=C_r(s)R(s)-C_y(s)Y(s), \quad (12)$$

represented as a block diagram in Fig. 1, where

$$C_r(s)=\frac{a_{0m}(Ts+1)}{b_0\,Ts},$$
$$C_y(s)=\frac{(v_1+Tv_2)\,\mathcal{W}_n(s)}{Ts\left(b_{n-1}s^{n-1}+\cdots+b_1s+b_0\right)} \quad (13)$$

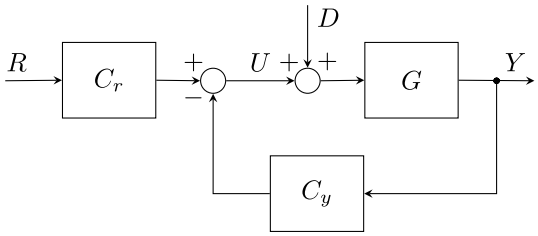

FIGURE 1. Block diagram of the 2-DOF structure.

where $\mathcal{W}_n(s)=\begin{bmatrix}1 & s & s^2 & \cdots & s^n\end{bmatrix}^T$ and

$$v_1=\begin{bmatrix}a_{0,m} & a_{1,m} & \cdots & a_{n-1,m} & 1\end{bmatrix},$$
$$v_2=\begin{bmatrix}0 & (a_{0,m}-a_0) & \cdots & (a_{n-1,m}-a_{n-1})\end{bmatrix} \quad (14)$$

Considering the plant to control (1) with the controller expression (12)-(13), the following transfer functions can be obtained:

$$G_{yr}(s)=\frac{Y(s)}{R(s)}=\frac{G(s)C_r(s)}{1+G(s)C_y(s)}=G_m(s)e^{-Ls},$$
$$G_{yd}(s)=\frac{Y(s)}{D(s)}=\frac{G(s)}{1+G(s)C_y(s)}=\frac{Ts}{Ts+1}G_m(s)e^{-Ls}, \quad (15)$$

where $G_{yr}(s)$ and $G_{yd}(s)$ are the transfer functions which relate the set-point and the disturbance with the output, respectively.

Note from $G_{yr}(s)$ that the transient response does not depend on the choice of the filter parameter T, but only on the selection of the coefficients a_{im}, $i=0,\ldots,n-1$. From $G_{yd}(s)$, it can be seen that the disturbance rejection capability can be improved by choosing the smallest possible T without affecting the tracking control performance, which is one of the key advantages of the proposed method. Nevertheless, small values of T may lead the system to instability in the presence of model uncertainties. The next section proposes an LMI based criterion to find the most suitable value of T with a reasonable trade-off between disturbance rejection and robustness.

B. EQUIVALENT 2-DOF PID

Consider a 2-DOF PID control scheme with a first-order lead-lag filter:

$$U(s)=PID_r(s)R(s)-PID_y(s)F(s)Y(s), \quad (16)$$

where

$$PID_r(s)=K_p\Big(\beta+\frac{1}{T_is}+\gamma T_ds\Big),$$
$$PID_y(s)=K_p\Big(1+\frac{1}{T_is}+T_ds\Big),$$
$$F(s)=\frac{\alpha s+1}{\tau s+1}. \quad (17)$$

being $R(s)\in\mathbb{R}$ the set-point reference signal. The parameters K_p, T_d and T_i are the proportional gain, derivative time and integral time, respectively, α and τ the lead-lag filter parameters, β and γ are the proportional and derivative set-point weights that only affect the tracking performance.

Note that (16) is reduced to a 1-DOF PID controller by setting $\beta = \gamma = 1$. Nevertheless, a common practice is to set $\gamma = 0$ when designing a 2-DOF PID in order to avoid high control actions in case of tracking non-smooth references [45].

From (12)-(13) and (16) with $\gamma = 0$, the following equivalence can be obtained by setting $PID_r(s) = C_r(s)$:

$$K_p\left(\beta + \frac{1}{T_i s}\right) = \frac{a_{0m}(Ts+1)}{b_0 Ts} \tag{18}$$

Matching the polynomial coefficients, the expressions for the PID parameters T_i and β given in Table 1 can be deduced as a function of the system parameters and $T, a_{im}, i = 0, 1$, which are independent of the order system and the delay L. Similarly, the rest of the PID parameters K_p, T_d, τ and α can be obtained from the equivalences given below, which are obtained by matching $PID_y(s)$ to $C_y(s)$ (or $PID_y(s)F(s)$ to $C_y(s)$) with the input delay approximated as a lag dynamics as $e^{-sL} \approx 1/(1+Ls)$. For first and second-order systems, the following equivalences can be obtained:

- First order plant ($T_d = 0, \tau = 0, \alpha = 0$):

$$K_p\left(1 + \frac{1}{T_i s}\right) = \frac{a_{0,m} + s(1 + T(a_{0m} - a_0))}{Tb_0 s} \tag{19}$$

- First order plant with time delay ($\tau = 0, \alpha = 0$):

$$K_p\left(1 + \frac{1}{T_i s} + T_d s\right) = \frac{\left(a_{0,m} + s(1 + T(a_{0m} - a_0))\right)(1+Ls)}{Tb_0 s} \tag{20}$$

- Second order plant ($\alpha = 0$):

$$K_p\left(1 + \frac{1}{T_i s} + T_d s\right)\left(\frac{1}{\tau s + 1}\right) = \frac{a_{0,m} + s(a_{1m} + T\,(a_{0m} - a_0))}{Tb_1 s^2 + Tb_0 s} \tag{21}$$

$$+ \frac{s^2(1 + T\,(a_{1m} - a_1))}{Tb_1 s^2 + Tb_0 s} \tag{22}$$

- Second order plant with time delay:

$$K_p\left(1 + \frac{1}{T_i s} + T_d s\right)\left(\frac{\alpha s + 1}{\tau s + 1}\right) = \frac{a_{0,m} + s(a_{1m} + T\,(a_{0m} - a_0))}{Tb_1 s^2 + Tb_0 s} \tag{23}$$

$$+ \frac{s^2(1 + T\,(a_{1m} - a_1))\,(1+Ls)}{Tb_1 s^2 + Tb_0 s} \tag{24}$$

Table 1 summarizes the equivalent expressions for each parameter and the representative plant models.

Remark 1: For non-minimum phase processes, i.e., a positive zero in the controlled plant, the proposed method cannot be directly applied. To solve this, the non-minimum phase dynamics can be approximated as a time delay [46] or simply treated as a unknown disturbance.

Remark 2: Although first-order or second-order systems are only considered for the equivalence of PID controller parameters given in Table 1, higher-order systems can also be included in our analysis by applying approximation methods based on reduction model approaches. This is a common practice in many control applications [47], where most processes are identified as first or second-order directly [48] or approximated in the frequency range of interest [49]. On the other hand, the delay L in (1) makes it possible to deal with higher order systems using the Pade approximation technique [46] and further include the presence of input and output delays in the control loop.

Remark 3: Note that the proposed method is applicable to a 2-DOF PID control scheme, where the set-point tracking control only depends on the choice of the coefficients a_{mi} through the desired eigenvalues of A_m in (4). Hence, the filter parameter T can be used to adjust the trade-off between robustness and disturbance rejection without affecting the set-point tracking response.

IV. TRADE-OFF BETWEEN DISTURBANCE REJECTION AND ROBUSTNESS

This section offers a guide to determine the value of T in order to reach a trade-off between disturbance rejection and robustness against model uncertainties. The system performance is usually evaluated by means of the integral absolute error (IAE) [1], defined by $\text{IAE} = \int_0^\infty |e(t)|dt$ with respect to any of the possible system inputs. In particular, the disturbance rejection performance can be evaluated as the IAE when a unitary step in the disturbance is introduced and $r(t) = 0$, which can be simply computed as:

$$\text{IAE}_d = \lim_{s\to 0} \frac{1}{s} G_{yd}(s) = \frac{T_i}{K_p} = \frac{b_0 T}{a_{0m}} \tag{25}$$

assuming that the response of G_{yd} does not exhibit overshoot (this is guaranteed if the poles of $G_m(s)$ are real) or in case of small overshoot values. From (25), it is easily deduced that T should be chosen as small as possible in order to increase the disturbance rejection performance.

Robustness can be evaluated by the classic robustness margins [50], i.e., the gain margin (GM), the phase margin (PM) and the delay margin (DM), which are defined as

$$GM = \frac{1}{|L(j\omega_{180^\circ})|},$$
$$PM = 180^\circ - \angle L(j\omega_{cr}),$$
$$DM = \frac{PM}{\omega_{cr}},$$

where $L(j\omega) = PID_y(j\omega)F(jw)G(j\omega)$ and ω_{cr}, ω_{180° are defined such that $|L(j\omega_{cr})| = 1$ and $\angle L(j\omega_{180^\circ}) = 180^\circ$, respectively. These indexes refer to the gain, phase and time delay which could be introduced before the system becomes unstable.

Other relevant performance indices are the integral of time-multiplied absolute-value of error (ITAE) [51], the root mean square error (RMSE) [51] and the Total Variation (TV) [28]. The ITAE and RMSE are employed to evaluate the set-point tracking performance, while the TV is used to measure the control efforts (manipulated input usage) or smoothness of the control signal. These indices are defined

TABLE 1. Equivalence of PID controller parameters for first and second-order systems.

Model	K_p	T_d	T_i	β	τ	α
$\frac{b_0}{s+a_0}$	$\frac{a_{0m}-a_0+1/T}{b_0}$	—	$\frac{K_pTb_0}{a_{0m}}$	$\frac{a_{0m}}{b_0K_p}$	—	—
$\frac{b_0}{s+a_0}e^{-Ls}$	$\frac{a_{0m}-a_0+1/T+La_{0m}/T}{b_0}$	$\frac{(a_{0m}-a_0+1/T)L}{b_0K_p}$	$\frac{K_pTb_0}{a_{0m}}$	$\frac{a_{0m}}{b_0K_p}$	—	—
$\frac{b_1s+b_0}{s^2+a_1s+a_0}$	$\frac{a_{0m}-a_0+a_{1m}/T}{b_0}$	$\frac{a_{1m}-a_1+1/T}{b_0K_p}$	$\frac{K_pTb_0}{a_{0m}}$	$\frac{a_{0m}}{b_0K_p}$	$\frac{b_1}{b_0}$	—
$\frac{b_1s+b_0}{s^2+a_1s+a_0}e^{-Ls}$	$\frac{a_{0m}-a_0+a_{1m}/T}{b_0}$	$\frac{a_{1m}-a_1+1/T}{b_0K_p}$	$\frac{K_pTb_0}{a_{0m}}$	$\frac{a_{0m}}{b_0K_p}$	$\frac{b_1}{b_0}$	L

as: $ITAE = \int_0^t t\,|y_r - y|\,d\tau$; $RMSE = \sqrt{\frac{1}{t}\int_0^t (y_r-y)^2\,d\tau}$ and $TV = \sum_{i=1}^{i=\infty} |u_{i+1} - u_i|$. As in the IAE, the resulting error $|y_r - y|$ can be attributed to a set-point change or a disturbance, which will allow to evaluate the set-point tracking performance and the disturbance rejection independently.

On the other hand, with the objective of evaluating the closed-loop robust performance against time-varying parametric uncertainties on the system model, first consider the following state space realization of the plant $G(s)$ defined in (1):

$$\begin{aligned} \dot{x}(t) &= (A + \Delta_A(t))\,x(t) + (B + \Delta_B(t))\,(u(t) + d(t)), \\ y(t) &= Cx(t) \end{aligned} \tag{26}$$

where $A \in \mathcal{R}^{n\times n}$, $B \in \mathcal{R}^{n\times 1}$ and $C \in \mathcal{R}^{1\times n}$ are any set of system matrices such that $G(s)\frac{1}{Ls+1} = C\,(sI_n - A)^{-1}\,B$ where $G(s)$ is defined in (1), and all possible time-varying uncertainties in the system model (including those of the approximation error of delay $e^{-Ls} \approx 1/(Ls+1)$) are described by the classical norm-bounded form [52]:

$$(\Delta_A(t),\,\Delta_B(t)) = \mu G\Delta(t)\,(H_A,\ H_B) \tag{27}$$

where G, H_A, H_B are time-constant matrices of appropriate dimensions, $\Delta(t)$ is an unknown time-varying matrix satisfying $\Delta(t)^T\Delta(t) \le I,\ \forall t \ge 0$ and $\mu \ge 0$ is a scalar that determines the size of uncertainties. The state-space realization of $PID_y(s) = C_y(s)$ (see (13)) can be expressed as:

$$\begin{aligned} \dot{x}_c(t) &= A_c x_c(t) + B_c y(t), \\ u(t) &= C_c x_c(t) + D_c y(t) \end{aligned} \tag{28}$$

where $A_c \in \mathcal{R}^{n_c\times n_c}$, $B \in \mathcal{R}^{n_c\times 1}$ and $C \in \mathcal{R}^{1\times n_c}$ are any set of system matrices such that $PID_y(s) = C_y(s) = C_c\left(sI_{n_c} - A_c\right)^{-1}B_c + D_c$ where $C_y(s) = PID_y(s)$ is the proposed PID control scheme, and n_c is the order of the controller. From (26), (12) and (28), the closed-loop system with $r(t) = 0$ renders:

$$\begin{aligned} \dot{\bar{x}}(t) &= \bar{A}(t)\bar{x}(t) + \bar{B}(t)d(t), \\ y(t) &= \bar{C}\bar{x}(t) \end{aligned} \tag{29}$$

where $\bar{A}(t) = \bar{A} + \mu\bar{G}\Delta(t)\bar{H}$, $\bar{B}(t) = \bar{B} + \mu\bar{G}\Delta(t)H_B$, $\bar{C} = \begin{bmatrix} C & 0 \end{bmatrix}$, and

$$\begin{aligned} \bar{A} &= \begin{bmatrix} A - BD_cC & -BC_c \\ B_cC & A_c \end{bmatrix}, \quad \bar{B} = \begin{bmatrix} B \\ 0 \end{bmatrix}, \\ \bar{G} &= \begin{bmatrix} G \\ 0 \end{bmatrix}, \ \bar{H} = \begin{bmatrix} H_A - H_BD_cC & -H_BC_c \end{bmatrix}. \end{aligned} \tag{30}$$

The following theorem gives a sufficient condition based on Linear Matrix Inequalities (LMIs) [44] to ascertain the robust exponential stability of the resulting closed-loop system described above with guaranteed H_∞ disturbance rejection from the controlled output $y(t)$ and any disturbance signal $d(t)$ of bounded energy, that is to say, $\int_0^t y^T(s)y(s)ds \le \delta^2\int_0^t d^T(s)d(s)ds, \forall t > 0$, where δ is the L_2 induced gain from $d(t)$ to $y(t)$. It is worthwhile mentioning that LMIs can easily be solved by means of semidefinite-programming tools [44]. Indeed, efficient polynomial-time optimization algorithms (e.g., interior-point [53]) are available in standard commercial libraries, such as the LMI Control Toolbox [54] and SEDUMI [55].

Theorem 1: Given a prescribed level of H_∞ disturbance rejection δ, the closed-loop system (29) is robustly exponentially stable against all possible time-varying parametric uncertainties on the form (27) if there is a symmetric matrix $P = P^T \in \mathcal{R}^{n+n_c} > 0$ and scalars $\varepsilon > 0$, $\rho > 0$ such that the following LMI holds:

$$\begin{bmatrix} \bar{A}^TP + P\bar{A} & P\bar{B} & P\bar{G} & \bar{H}^T & \varepsilon\bar{C}^T \\ (*) & \varepsilon\delta^2 I & 0 & H_B^T & 0 \\ (*) & (*) & -\rho I & 0 & 0 \\ (*) & (*) & (*) & -I & 0 \\ (*) & (*) & (*) & 0 & -\varepsilon I \end{bmatrix} < 0 \tag{31}$$

Moreover, the size of uncertainties defined in (27) can be obtained as $\mu = \rho^{-1/2}$.

Proof: Consider the quadratic Lyapunov function candidate $V(t) = \bar{x}^T(t)P\bar{x}(t)$. Hence, the closed-loop system (29) is robustly exponentially stable with guaranteed H_∞ disturbance rejection from $y(t)$ to $d(t)$ if $\dot{V}(t) + y^T(t)y(t) - \delta^2\,d^T(t)d(t) < 0$, leading to the following condition:

$$\begin{aligned} &\dot{V}(t) + y^T(t)y(t) - \delta^2\,d^T(t)d(t) \\ &= \dot{\bar{x}}^T(t)P\bar{x}(t) + \bar{x}^T(t)P\dot{\bar{x}}(t) \\ &= \bar{x}^T(t)\left(\bar{A}^T(t)P + P\bar{A}(t) + \bar{C}^T\bar{C}\right)\bar{x}(t) \\ &\quad + \bar{x}^T(t)P\bar{B}(t)d(t) + d^T(t)\bar{B}^T(t)P\bar{x}(t) - \delta^2\,d^T(t)d(t) \\ &\quad \begin{bmatrix} \bar{x}^T(t) \\ d^T(t) \end{bmatrix}^T \begin{bmatrix} \bar{A}^T(t)P + P\bar{A}(t) + \bar{C}^T\bar{C} & P\bar{B}(t) \\ (*) & -\delta^2 I \end{bmatrix} \begin{bmatrix} \bar{x}(t) \\ d(t) \end{bmatrix} \\ &< 0 \end{aligned} \tag{32}$$

The condition (32) is true if and only if

$$\begin{bmatrix} \bar{A}^T(t)P + P\bar{A}(t) + \bar{C}^T\bar{C} & P\bar{B}(t) \\ (*) & -\delta^2 I \end{bmatrix} < 0,\ \forall t \ge 0.$$

Taking into account that $\bar{A}(t) = \bar{A} + \mu\bar{G}\Delta(t)\bar{H}$ and $\bar{B}(t) = \bar{B} + \mu\bar{G}\Delta(t)H_B$, the latter inequality renders:

$$\begin{bmatrix} \bar{A}^T P + P\bar{A} + \bar{C}^T\bar{C} & P\bar{B} \\ (*) & -\delta^2 I \end{bmatrix} + \begin{bmatrix} \mu P\bar{G} \\ 0 \end{bmatrix} \Delta(t) \begin{bmatrix} \bar{H} & H_B \end{bmatrix} + \begin{bmatrix} \bar{H}^T \\ H_B^T \end{bmatrix} \Delta^T(t) \begin{bmatrix} \mu\bar{G}^T P & 0 \end{bmatrix} < 0 \quad (33)$$

Applying Petersen's inequality [56], one has that $\forall\Delta(t)$ satisfying $\Delta(t)^T\Delta(t) \leq I$, the following inequality holds:

$$\begin{bmatrix} \mu P\bar{G} \\ 0 \end{bmatrix} \Delta(t) \begin{bmatrix} \bar{H} & H_B \end{bmatrix} + \begin{bmatrix} \bar{H}^T \\ H_B^T \end{bmatrix} \Delta^T(t) \begin{bmatrix} \mu\bar{G}^T P & 0 \end{bmatrix} \leq \varepsilon \begin{bmatrix} \mu P\bar{G} \\ 0 \end{bmatrix} \begin{bmatrix} \mu\bar{G}^T P & 0 \end{bmatrix} + \varepsilon^{-1} \begin{bmatrix} \bar{H}^T \\ H_B^T \end{bmatrix} \begin{bmatrix} \bar{H} & H_B \end{bmatrix} \quad (34)$$

Substituting (34) into (33), the following inequality is obtained:

$$\begin{bmatrix} \bar{A}^T P + P\bar{A} + \bar{C}^T\bar{C} & P\bar{B} \\ (*) & -\delta^2 I \end{bmatrix} + \varepsilon \begin{bmatrix} \mu P\bar{G} \\ 0 \end{bmatrix} \begin{bmatrix} \mu\bar{G}^T P & 0 \end{bmatrix} + \varepsilon^{-1} \begin{bmatrix} \bar{H}^T \\ H_B^T \end{bmatrix} \begin{bmatrix} \bar{H} & H_B \end{bmatrix} < 0 \quad (35)$$

Applying three times the Schur Complement [57], the above inequality (35) is true if the following matrix inequality holds:

$$\begin{bmatrix} \bar{A}^T P + P\bar{A} & P\bar{B} & \mu P\bar{G} & \bar{H}^T & \bar{C}^T \\ (*) & -\delta^2 I & 0 & H_B^T & 0 \\ (*) & (*) & -\varepsilon^{-1} I & 0 & 0 \\ (*) & (*) & (*) & -\varepsilon I & 0 \\ (*) & (*) & (*) & (*) & -I \end{bmatrix} < 0 \quad (36)$$

From the congruence transformation obtained by pre- and post-multiplying the above matrix inequality by $diag\left(I, I, \mu^{-1}I, \varepsilon^{-1}I, I\right)$ and defining $\tilde{P} = \varepsilon P$, it is obtained

$$\begin{bmatrix} \varepsilon^{-1}\bar{A}^T\tilde{P} + \varepsilon^{-1}\tilde{P}\bar{A} & \varepsilon^{-1}\tilde{P}\bar{B} & \varepsilon^{-1}\tilde{P}\bar{G} & \varepsilon^{-1}\bar{H}^T & \bar{C}^T \\ (*) & -\delta^2 I & 0 & \varepsilon^{-1}H_B^T & 0 \\ (*) & (*) & -\varepsilon^{-1}\mu^{-2}I & 0 & 0 \\ (*) & (*) & (*) & -\varepsilon^{-1}I & 0 \\ (*) & (*) & (*) & (*) & -I \end{bmatrix} < 0 \quad (37)$$

Finally, pre- and post-multiplying the above matrix inequality by $diag\left(\varepsilon^{1/2}I, \varepsilon^{1/2}I, \varepsilon^{1/2}I, \varepsilon^{1/2}I, \varepsilon^{1/2}I\right)$ and renaming $P = \tilde{P}$, $\rho = \mu^{-2}$, the above inequality is proven to be equivalent to LMI (31), concluding the proof. □

Remark 4: Given a prescribed H_∞ disturbance rejection δ, the maximum tolerance against model uncertainties can easily be determined by solving the convex optimization problem $\bar{\rho} = min\ \rho$ s.t LMI (31), where $\bar{\mu} = \bar{\rho}^{-1/2}$. This result will be used to compare the robust performance of the different PID control designs with the proposed one.

Remark 5: One of the advantages of the proposed method is that the existing trade-off between disturbance rejection and robustness can easily be adjusted by tuning a single scalar parameter (namely T) taking into account the disturbance indices *IAE* and δ, and some of the robustness indices defined above: $\bar{\mu}$, GM, PM or DM. In particular, given a prescribed value for H_∞ disturbance rejection δ, the convex optimization problem described in Remark 3 and Theorem 1, in combination with dichotomic search in T, is helpful to find the best choice for T such that the tolerance against time-varying model uncertainties in $\bar{\mu}$ is maximized.

V. EXAMPLES

This section provides three comparative examples aimed at showing the effectiveness of the proposed method and the improvements with respect to other existing PID tuning methods.

Note that $C_r(s)$ in (13) is always a PI-like control scheme, but $C_y(s)$ is a full PID structure. Hence, in order to ensure that $PID_y(s)$ is realizable, the following PID with a derivative filter has been used in the examples.

$$PID(s) = K_p\left(1 + \frac{1}{T_i s} + \frac{T_d s}{NT_d s + 1}\right). \quad (38)$$

A. EXAMPLE 1

Consider the following FOPTD plant consisting in a spherical tank system [58]:

$$G(s) = \frac{3.6215}{330.46s + 1} e^{-11.7s},$$

Applying the approximation $e^{-11.7\,s} \approx 1/(11.7s + 1)$, a state-space representation as (26) of the above system can be obtained with system matrices

$$A = \begin{bmatrix} 0 & 1 \\ -0.00026 & -0.0885 \end{bmatrix}, B = \begin{bmatrix} 0 \\ 0.00094 \end{bmatrix}, C = \begin{bmatrix} 1 & 0 \end{bmatrix}$$

and model uncertainties are described by (27) with matrices $G = \mu\begin{bmatrix} 1 \\ 1 \end{bmatrix}$, $H_A = \begin{bmatrix} 1 & 1 \end{bmatrix}$ and $H_B = 1$. The above state-space representation will be useful to compare the robust performance of different control designs via Theorem 1 and Remark 4 by maximizing the size of uncertainties μ.

A 2-DOF PID control design with $K_p = 3.067$, $T_d = 0.48$, $T_i = 37$, $\beta = 0.16$ and $\gamma = 0.11$ is obtained by applying a heuristic method for control design in [58]. Both PID will use a derivative filter of $N = 0.1$.

For the control design, a similar closed-loop settling time (about 200s) is established, which correspond to a $a_{0m} = b_{0m} = 0.02$. The filter parameter T is obtained to guarantee the same disturbance rejection performance in terms of IAE_d (25) as [58]. Hence, it is obtained (25) that $T = 30.91$. Note that the plant model corresponds to the second row in Table 1, leading to the PID controller parameters: $K_p = 5.17$, $T_d = 10.14$, $T_i = 87.98$, $\beta = 0.35$ and $\gamma = 0$.

TABLE 2. Disturbance rejection and robustness performance indices for Example 1, Example 2 and Example 3.

Controller	$\bar{\mu}$	GM	$PM(^\circ)$	DM	TV	Set-point IAE	Set-point $ITAE$	Set-point $RMSE$	Disturbance IAE_d^*	Disturbance $ITAE$	Disturbance $RMSE$
*Example*1											
$H-2PID$	0.0037	3.59	34.17	14.84	6.25	54.4	3221	2.94	17.05	1566	0.18
Proposed	0.0105	1.62	75.18	21.03	9.45	61.7	2575	2.92	16.50	1253	0.24
*Example*2											
AMIGO	0.0215	5.70	54	2.29	2.73	5.06	15.7	2.55	2.35	13.9	0.43
Proposed	0.0695	5.63	70	2.79	1.81	5.02	15.6	2.52	2.32	13.2	0.39
*Example*3											
LQR synth.	0.0909	0.55	22	0.25	12.20	5.06	14.2	2.51	5.94	24.3	1.70
Proposed	0.2016	0.55	24.35	0.30	4.64	3.51	10.4	2.39	5.91	19.5	1.48

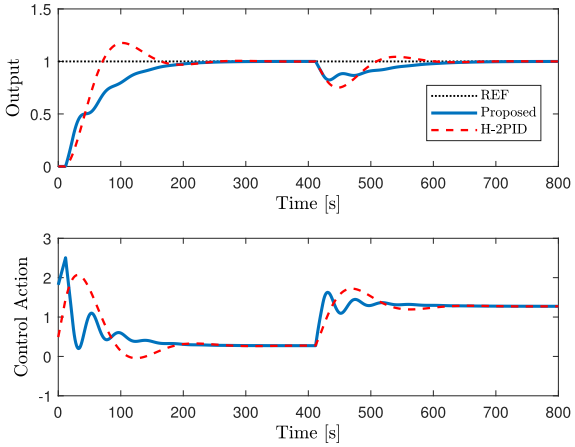

FIGURE 2. Simulation of Example 1.

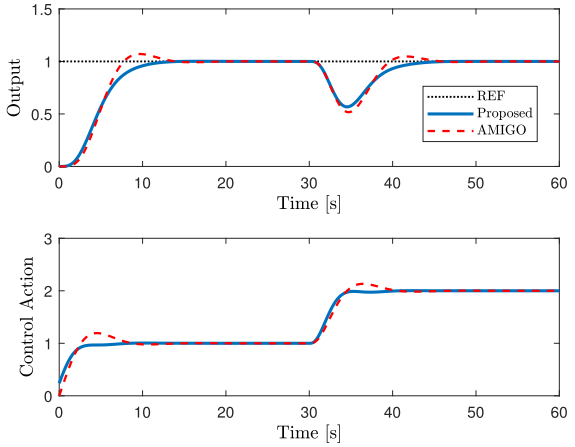

FIGURE 3. Simulation of Example 2.

Table 2 shows the IAE_d from (25) computed from the simulation results (namely IAE_d^*), with H_∞ disturbance rejection $\delta = 1$. Note the value is not exactly $IAE_d = 17$ due to the model approximation, i.e. delay dynamics. Table 2 also depicts the robustness and performance indices defined in Section IV corresponding to both control designs: $\bar{\mu}$, PM, GM, $ITAE$, $RMSE$ and TV.

A comparative time-evolution of the closed-loop system state with both controllers is depicted in Fig. 2. A step increment of 1 in the reference signal $r(t)$ has been introduced at the beginning of the simulation. Moreover, a step disturbance signal $d(t)$ of -1 has been induced at time instant 400s. It can be appreciated that the settling time is around 200s in both cases, as expected from the closed-loop specifications. However, it can also be noted that the proposed control (blue dashed-line) achieves a better transient response with less overdamping than the previous design (red dash-dotted line). This fact shows that the proposed control is more robust against the model uncertainties derived from the approximation error of the delay term $e^{-11.7s}$.

B. EXAMPLE 2

The balanced lag and delay process proposed in [25] has the following fourth-order transfer function:

$$G(s) = \frac{1}{(s+1)^4},$$

An approximated SOPTD model of the above system can be obtained as:

$$G_2(s) = \frac{0.67}{s^2 + 1.67s + 0.67} e^{-1.5s},$$

using the *half rule*, a simple reduction model method explained in detail in [28].

A 2-DOF PID control design with $K_p = 1.12$, $T_d = 0.71$, $T_i = 2.40$, $\beta = 0$ and $\gamma = 0$ is obtained by means of the AMIGO method in [25]. As in the previous example, the set-point tracking and disturbance rejection have been selected similar to the previous design: a settling time around $10s$ and $IAE_d = 2.35$. From these specifications, we obtain (25) in which $T = 0.85$. Note that the plant model in this example corresponds to the fourth row in Table 1, obtaining the 2-DOF PID controller parameters: $K_p = 1.37$, $T_d = 0.996$, $T_i = 3.21$, $\beta = 0.175$, $\alpha = 1.5$ and $\tau = 0$. Both controllers have a derivate filter of $N = 0.01$.

Simulations are shown in Fig. 3. A unitary step reference signal $r(t)$ has been introduced at the beginning of the simulation. Also, a step disturbance signal $d(t)$ of amplitude equal to -1 has been introduced at time instant 30s. As it can be seen in the Figure, a better transient response (less overshot) is achieved by the proposed control design.

Table 2 summarizes the comparative indices of the second example for a H_∞ disturbance rejection index $\delta = 1$. As in the previous example, it shows better tolerance against model

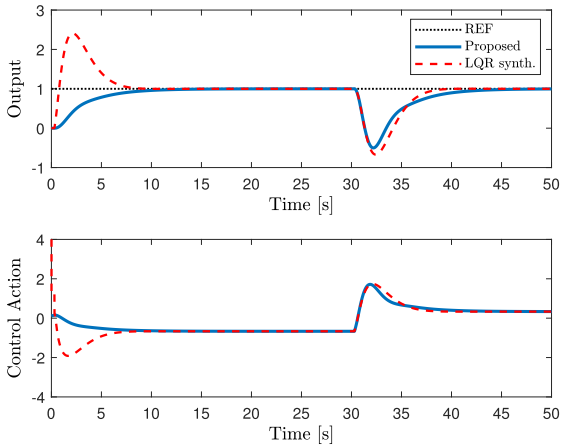

FIGURE 4. Simulation of Example 3.

uncertainties coming from the phase and time-delay model errors.

C. EXAMPLE 3

In this example, the following unstable plant with time-delay studied in [59] is considered:

$$G_3(s) = \frac{1.5}{(0.5s+1)(s-1)}e^{-0.3s}$$

In [59], an optimal PID tuning via LQR for SOPTD is presented. For this plant, it yields the parameters $K_p = 1.22$, $T_d = 0.47$, $T_i = 7.20$, $\beta = 1$ and $\gamma = 1$. As in the previous examples, tracking and disturbance rejection performance have been selected similar to the previous design with LQR: a settling time around $10s$ and $IAE_d = 5.9$. Then, from (25), it is obtained that $T = 0.64$. Note that the plant model in this example corresponds to the fourth row in Table 1, obtaining the PID controller parameters: $K_p = 1.37$, $T_d = 0.41$, $T_i = 8.10$, $\beta = 0.08$, $\alpha = 0.3$ and $\tau = 0$. The derivative filter is $N = 0.01$ for both PID.

The comparative indices for the third example are presented in Table 2, with H_∞ disturbance rejection $\delta = 3$. In Fig. 4, the closed-loop dynamics of both controllers (proposed vs LQR) is compared. Here, a unitary step reference signal $r(t)$ has been introduced at the beginning of the simulation. Also, a step disturbance signal $d(t)$ of amplitude equal to -1 has been introduced at time instant 30s. When the reference change is introduced, the LQR synthesis shows a considerable overshoot on the system response while the proposed tuning does not. As above pointed out, this is produced by the non-zero value of the γ PID parameter. Regarding the disturbance rejection performance, it can be observed a similar performance with a slight reduction of the peak value with the proposed method.

VI. EXPERIMENTAL RESULTS

The proposed solution has been implemented in the 3DOF Hover of Quanser shown in Fig. 5. This experimental platform consists of a quadrotor installed in a pivot joint. Therefore, it can freely spin in roll, pitch and yaw angles.

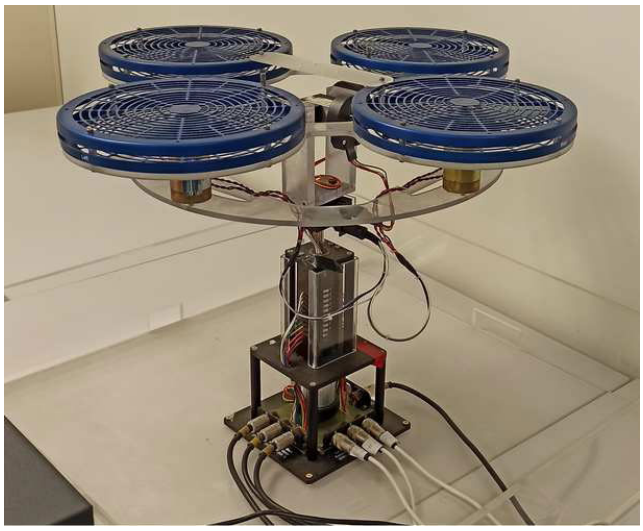

FIGURE 5. 3DOF Hover of Quanser.

TABLE 3. Controller parameters designed for the experimental results.

Controller	IAE_d	K_p	T_d	T_i	β	α
$LQR\ synth.$	0.0015	113.7	0.32	1.84	0	–
$Prop.\ T = 0.26$	0.015	117.8	0.55	1.77	0.15	0.12
$Prop.\ T = 0.13$	0.0075	217.8	0.47	1.63	0.08	0.12
$Prop.\ T = 0.39$	0.0225	84.4	0.61	1.90	0.21	0.12

The angles are measured by optical encoders with an accuracy of 0.04 degrees, and the control inputs of the system are the voltages applied to the four motors, which can range between $-10V$ and 10V. The designed control strategy has been executed on a PC with a real-time Linux distribution, which makes it perfectly possible to run the full algorithm with a sampling time of 0.01 sec. The computer is connected to the Quanser hardware by means of a data acquisition board.

The quadrotor could be seen as a decoupled system with each axis modeled as a double integrator [36]. If the additional dynamics introduced by the motors and sensors were considered, they could be approximated to a constant time delay [60]. In addition, the real system has some additional dynamics not included in the system model, such as parameter uncertainty or nonlinear dynamics. Nevertheless, close to the equilibrium point, such extra dynamics can be considered as a time-constant disturbance. Hence, the model of the Quanser platform is

$$G(s) = \frac{0.1}{s^2}e^{-0.12s},$$

where input and output signals are expressed in volts (V) and radians (rad), respectively. Analogously to previous examples, by applying the approximation $e^{-0.12\,s} \approx 1/(0.12s+1)$, a state-space representation as (26) of the above plant system model $G(s)$ can be obtained with system matrices

$$A = \begin{bmatrix} 0 & 1 & 0 \\ 0 & 0 & 1 \\ 0 & 0 & -8.33 \end{bmatrix}, \quad B = \begin{bmatrix} 0 \\ 0 \\ 0.833 \end{bmatrix}, \quad C = \begin{bmatrix} 1 & 0 & 0 \end{bmatrix}$$

and model uncertainties are described by (27) with matrices $G = \mu\begin{bmatrix} 1 & 1 & 1 \end{bmatrix}^T$, $H_A = \begin{bmatrix} 1 & 1 & 1 \end{bmatrix}$ and $H_B = 1$.

TABLE 4. Disturbance rejection and robustness performance indices for the experimental results.

Controller	$\bar{\mu}$	GM	$PM(^\circ)$	DM	TV	Set-point			Disturbance		
						IAE	$ITAE$	$RMSE$	IAE_d^*	$ITAE$	$RMSE$
$LQR\ synth.$	0.0063	0.149	51	0.20	141	59.1	2058	6.46	4.68	10.8	2.29
$Prop.\ T = 0.26$	0.0064	0.082	74	0.20	158	50.1	1734	6.02	4.36	9.48	1.98
$Prop.\ T = 0.13$	0.0032	0.060	78	0.13	239	43.7	1442	5.76	2.19	4.25	1.16
$Prop.\ T = 0.39$	0.0090	0.11	72	0.24	133	56.2	2023	6.23	6.48	15.6	2.64

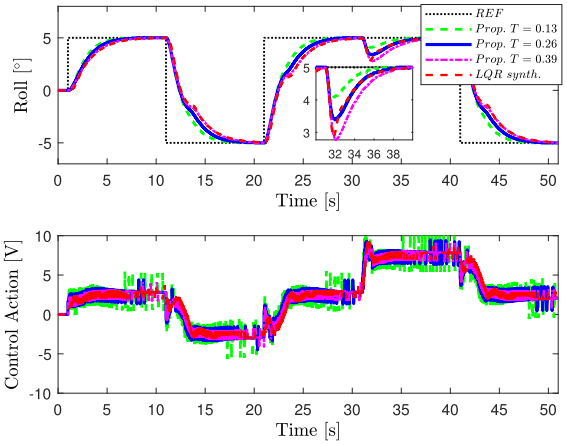

FIGURE 6. Experimental results.

The above state-space representation will be useful to compare the robust performance of different control designs via Theorem 1 and Remark 4 by maximizing the size of uncertainties μ (see $\bar{\mu}$ in Table 4).

In [61], authors proposed an extension of [59] to deal with different integrator systems with time-delay. Contrary to [25], [58], [59], this methodology explicitly includes the double integrator as a particular case, so it will be used here for a fair comparison. Following the methodology given in [61] applied to the Quanser platform above described, a stabilizing 2-DOF PID control with $K_p = 113.7$, $T_d = 0.32$, $T_i = 1.84$, $\beta = 0$ and $\gamma = 0$ is designed. As in the previous examples, a similar closed-loop settling time (about 3s) is established. The filter parameter T is obtained to guarantee the same disturbance rejection performance in terms of IAE_d. For instance, given $IAE_d = 0.015$, it can be deduced from (25) that $T = 0.26$. Hence, the 2-DOF PID controller parameters $K_p = 117.8$, $T_d = 0.55$, $T_i = 1.77$, $\beta = 0.15$, $\alpha = 0.12$ and $\tau = 0$ are designed taking into account the expressions given in the fourth row of Table 1.

To show the effect of the tuning parameter T on the closed-loop system performance, we set $T = 0.13$, $T = 0.26$ and $T = 0.39$, leading to a more aggressive control in the first case and a smoother control in the third case. In all controller designs, the same settling-time specifications of the previous comparative studies have been considered, together with a H_∞ disturbance rejection $\delta = 1$ and the choice $N = 0.1$. The obtained control parameters are summarized in Table 3.

For experimental essays, different set-points variations are established: a set-point change of 5 degrees at time instants $1s$ and $21s$, a negative -5 degree step at $11s$ and $41s$, and a step disturbance of amplitude -5V at 31s (see black-dotted line in Fig. 6). Table 4 and Fig. 6 show respectively the comparative indices and time evolution of the roll angle and control action for the experimental results. For the IAE_d, note that the angular magnitudes are expressed in radian units, but they are expressed in degrees for the sake of readability in Table 4 and Fig. 6.

Here, it can be observed a slightly faster response by the proposed method ($T = 0.26$) and a softer response on disturbance rejection. The performance indices show, except for GM and TV, that the proposal can deal with a wider variety of uncertainties, such as those coming from the phase and time delay modeling, as well as external disturbances.

As can be seen in Fig. 6, the three proposed experiments have similar transient responses for set-point tracking. This is due to the fact that the three design have considered a settling time of $3s$. However, there exists a little difference between them in the achieved performance due to the intrinsic disturbances that affect the system, which lead the more aggressive designed controller with $T = 0.13$ to achieve a set-point response more similar to the nominal case. Consequently, the best disturbance rejection response is achieved for $T = 0.13$, and the worst transient response is obtained for $T = 0.39$. Regarding the control action, it exhibits the worst behavior (higher TV) for $T = 0.13$, and the best one for $T = 0.39$. This fact confirms the existing trade-off between the disturbance rejection IAE_d and TV which only depends on the choice of the parameter T. Note also from 4 that the IAE_d experimentally obtained (namely IAE_d^*) is approximately proportional to T, as it can be deduced from (25). Note also from Table 4 the trade-off between disturbance rejection and robustness, that is to say, better disturbance rejection (lower values for IAE_d^*) leads to worse robust performance.

VII. CONCLUSION AND PERSPECTIVES

A single-parameter 2-DOF PID tuning approach based on an Uncertainty and Disturbance Estimator (UDE) has been proposed. A general procedure to obtain the 2-DOF PID parameters, as well as the proper selection of the single parameter, has been shown. The key aspect of the proposed method is that the 2-DOF PID parameters can be obtained from the desired set-point settling time and tuning a single parameter, which can be obtained from the disturbance rejection index IAE_d or a certain robustness margin for time-varying parametric uncertainties by means of LMIs, without needing any complex numerical optimization. Therefore, the disturbance rejection and robust performance trade-off can be

easily settled. The proposed method is presented for first and second-order systems with time-delay, including unstable plants, although it is shown that this method can be applied to higher order systems, since the proposed method can deal with the ignored extra-dynamics of the plant system by treating it as a disturbance.

Simulations and experimental essays have been carried out. Three academic examples have been simulated in order to compare the proposed approach with three well-known classic tuning methods: (2-DOF PID with heuristic-based algorithms for tuning parameters, AMIGO and LQR synthesis methods). In all cases, it has been shown that better disturbance rejection can be achieved keeping a similar robust performance. A test-bed quadrotor platform was used to validate the controller presented. Future works could consider the use of the proposal with a self-tuning regulator, or be able to deal with larger time-delays by including predictor-feedback delay compensation approaches.

ACKNOWLEDGMENT

The authors would like to thank the Associate Editor and anonymous Reviewers for their constructive comments.

REFERENCES

[1] K. J. Åström, T. Hägglund, and K. J. Astrom, *Advanced PID Control*, vol. 461. Pittsburgh, PA, USA: ISA, 2006.

[2] T. L. Blevins, "PID advances in industrial control," *IFAC Proc. Volumes*, vol. 45, no. 3, pp. 23–28, 2012.

[3] T. Samad, "A survey on industry impact and challenges thereof [technical activities]," *IEEE Control Syst. Mag.*, vol. 37, no. 1, pp. 17–18, Feb. 2017.

[4] Y. Li, K. H. Ang, and G. C. Y. Chong, "PID control system analysis and design," *IEEE Control Syst.*, vol. 26, no. 1, pp. 32–41, Feb. 2006.

[5] J. G. Ziegler and N. B. Nichols, "Optimum settings for automatic controllers," *J. Dyn. Syst., Meas., Control*, vol. 115, no. 2B, pp. 220–222, Jun. 1993.

[6] B. D. Tyreus and W. L. Luyben, "Tuning PI controllers for integrator/dead time processes," *Ind. Eng. Chem. Res.*, vol. 31, no. 11, pp. 2625–2628, Nov. 1992.

[7] M. R. Matausek and T. B. Šekara, "PID controller frequency-domain tuning for stable, integrating and unstable processes, including dead-time," *J. Process Control*, vol. 21, no. 1, pp. 17–27, Jan. 2011.

[8] S. Das, K. Halder, and A. Gupta, "Delay handling method in dominant pole placement based PID controller design," *IEEE Trans. Ind. Informat.*, vol. 16, no. 2, pp. 980–991, Feb. 2020.

[9] M. Cetin and S. Iplikci, "A novel auto-tuning PID control mechanism for nonlinear systems," *ISA Trans.*, vol. 58, pp. 292–308, Sep. 2015.

[10] K. Bingi, R. Ibrahim, M. N. Karsiti, and S. M. Hassan, "Fractional order set-point weighted PID controller for pH neutralization process using accelerated PSO algorithm," *Arabian J. Sci. Eng.*, vol. 43, no. 6, pp. 2687–2701, Jun. 2018.

[11] K. Bingi, R. Ibrahim, M. N. Karsiti, S. M. Hassan, and V. R. Harindran, "Real-time control of pressure plant using 2DOF fractional-order PID controller," *Arabian J. Sci. Eng.*, vol. 44, no. 3, pp. 2091–2102, Mar. 2019.

[12] K. Bingi, R. Ibrahim, M. N. Karsiti, S. M. Hassan, and V. R. Harindran, "Fractional-order set-point weighted controllers," in *Fractional-Order Systems and PID Controllers*. Cham, Switzerland: Springer, 2020, pp. 9–100.

[13] R. Hotchi, H. Chibana, T. Iwai, and R. Kubo, "Active queue management supporting TCP flows using disturbance observer and smith predictor," *IEEE Access*, vol. 8, pp. 173401–173413, 2020.

[14] Z. Chen, Y. Yuan, X. Yuan, Y. Huang, X. Li, and W. Li, "Application of multi-objective controller to optimal tuning of PID gains for a hydraulic turbine regulating system using adaptive grid particle swam optimization," *ISA Trans.*, vol. 56, pp. 173–187, May 2015.

[15] A. Maitra, A. Senapati, S. Chatterjee, B. Bhattacharya, A. K. Kashyap, B. K. Mondal, and S. Ghosh, "Observing the effect of particle swarm optimization algorithm based PID controller," *J. Mech. Continua Math. Sci.*, vol. 13, no. 2, pp. 126–137, Jun. 2018.

[16] Z.-Y. Nie, C. Zhu, Q.-G. Wang, Z. Gao, H. Shao, and J.-L. Luo, "Design, analysis and application of a new disturbance rejection PID for uncertain systems," *ISA Trans.*, vol. 101, pp. 281–294, Jun. 2020.

[17] A. Leva and S. Seva, "Structure-specific analytical PID tuning for load disturbance rejection," *IFAC-PapersOnLine*, vol. 51, no. 4, pp. 137–142, 2018.

[18] H. Taguchi and M. Araki, "Two-degree-of-freedom PID controllers—Their functions and optimal tuning," *IFAC Proc. Volumes*, vol. 33, no. 4, pp. 91–96, Apr. 2000.

[19] M. Araki and H. Taguchi, "Two-degree-of-freedom PID controllers," *Int. J. Control, Automat., Syst.*, vol. 1, no. 4, pp. 401–411, 2003.

[20] S. Yamamoto, H. Hirahara, A. Tanaka, and T. Ara, "Simple robust design of two-degree-of-freedom PID controller for tracking drives of linear servo motors," in *Proc. 15th Int. Conf. Electr. Mach. Syst. (ICEMS)*, 2012, pp. 1–6.

[21] X. Wang, X. Yan, D. Li, and L. Sun, "An approach for setting parameters for two-degree-of-freedom PID controllers," *Algorithms*, vol. 11, no. 4, p. 48, Apr. 2018.

[22] M. Viteckova and A. Vitecek, "Standard, parallel and series two degree of freedom PID controllers," in *Proc. 20th Int. Carpathian Control Conf. (ICCC)*, May 2019, pp. 1–4.

[23] K. Bingi, R. Ibrahim, M. N. Karsiti, S. M. Hassan, and V. R. Harindran, "A comparative study of 2DOF PID and 2DOF fractional order PID controllers on a class of unstable systems," *Arch. Control Sci.*, vol. 28, no. 4, pp. 635–682, 2018.

[24] V. Kumar and S. Suhag, "Comparative analysis of salp swarm algorithm tuned 2-DOF PID and PIDF controllers for reducing the current consumption in EPAS system of electric vehicles," in *Proc. IEEE Students Conf. Eng. Syst. (SCES)*, Jul. 2020, pp. 1–6.

[25] K. J. Åström and T. Hägglund, "Revisiting the Ziegler–Nichols step response method for PID control," *J. Process Control*, vol. 14, no. 6, pp. 635–650, Sep. 2004.

[26] D. E. Rivera, M. Morari, and S. Skogestad, "Internal model control: PID controller design," *Ind. Eng. Chem. Process Des. Develop.*, vol. 25, no. 1, pp. 252–265, Jan. 1986.

[27] U. M. Nath, C. Dey, and R. K. Mudi, "Review on IMC-based PID controller design approach with experimental validations," *IETE J. Res.*, pp. 1–21, Feb. 2021.

[28] S. Skogestad, "Simple analytic rules for model reduction and PID controller tuning," *J. Process Control*, vol. 13, no. 4, pp. 291–309, Jun. 2003.

[29] R. P. Borase, D. Maghade, S. Sondkar, and S. Pawar, "A review of PID control, tuning methods and applications," *Int. J. Dyn. Control*, pp. 1–10, Jul. 2020.

[30] Q. Jin, Y. Shi, Q. Liu, M. Chu, and Y. Zhang, "Graphical robust PID tuning for disturbance rejection satisfying multiple objectives," *Chem. Eng. Commun.*, vol. 205, no. 12, pp. 1701–1711, Dec. 2018.

[31] P.-J. Ko and M.-C. Tsai, "H_∞ control design of PID-like controller for speed drive systems," *IEEE Access*, vol. 6, pp. 36711–36722, 2018.

[32] L. Guo and S. Cao, "Anti-disturbance control theory for systems with multiple disturbances: A survey," *ISA Trans.*, vol. 53, no. 4, pp. 846–849, Jul. 2014.

[33] A. Mohammadi, M. Tavakoli, H. J. Marquez, and F. Hashemzadeh, "Nonlinear disturbance observer design for robotic manipulators," *Control Eng. Pract.*, vol. 21, no. 3, pp. 253–267, Mar. 2013.

[34] J. Du, X. Hu, M. Krstić, and Y. Sun, "Robust dynamic positioning of ships with disturbances under input saturation," *Automatica*, vol. 73, pp. 207–214, Nov. 2016.

[35] X. Liu, Z. Liu, J. Shan, and H. Sun, "Anti-disturbance autopilot design for missile system via finite time integral sliding mode control method and nonlinear disturbance observer technique," *Trans. Inst. Meas. Control*, vol. 38, no. 6, pp. 693–700, Jun. 2016.

[36] A. Castillo, R. Sanz, P. Garcia, W. Qiu, H. Wang, and C. Xu, "Disturbance observer-based quadrotor attitude tracking control for aggressive maneuvers," *Control Eng. Pract.*, vol. 82, pp. 14–23, Jan. 2019.

[37] J. Betancourt, V. Balaguer, P. Castillo, P. García, and R. Lozano, "Robust linear control scheme for nonlinear aerial systems: An experimental study on disturbance rejection," in *Proc. IEEE 23rd Int. Conf. Intell. Transp. Syst. (ITSC)*, Sep. 2020, pp. 1–6.

[38] S. Li, J. Yang, W.-H. Chen, and X. Chen, "Generalized extended state observer based control for systems with mismatched uncertainties," *IEEE Trans. Ind. Electron.*, vol. 59, no. 12, pp. 4792–4802, Dec. 2012.
[39] A. Gonzalez, V. Balaguer, P. Garcia, and A. Cuenca, "Gain-scheduled predictive extended state observer for time-varying delays systems with mismatched disturbances," *ISA Trans.*, vol. 84, pp. 206–213, Jan. 2019.
[40] A. González, A. Cuenca, V. Balaguer, and P. García, "Event-triggered predictor-based control with gain-scheduling and extended state observer for networked control systems," *Inf. Sci.*, vol. 491, pp. 90–108, Jul. 2019.
[41] J. Han, "From PID to active disturbance rejection control," *IEEE Trans. Ind. Electron.*, vol. 56, no. 3, pp. 900–906, Mar. 2009.
[42] Q.-C. Zhong and D. Rees, "Control of uncertain LTI systems based on an uncertainty and disturbance estimator," *J. Dyn. Syst., Meas., Control*, vol. 126, no. 4, pp. 905–910, Dec. 2004.
[43] V. Balaguer, R. Sanz, P. Garcia, and P. Albertos, "Two-degree-of-freedom PID tuning based on an uncertainty and disturbance estimator," in *Proc. 7th Int. Conf. Syst. Control (ICSC)*, Oct. 2018, pp. 424–429.
[44] S. Boyd, L. E. Ghaoui, E. Feron, and V. Balakrishnan, *Linear Matrix Inequalities in System and Control Theory*, vol. 15. Philadelphia, PA, USA: SIAM, 1994.
[45] V. M. Alfaro, R. Vilanova, and O. Arrieta, "Considerations on set-point weight choice for 2-DoF PID controllers," *IFAC Proc. Volumes*, vol. 42, no. 11, pp. 721–726, 2009.
[46] Y. Shamash, "Model reduction using the routh stability criterion and the Padé approximation technique," *Int. J. Control*, vol. 21, no. 3, pp. 475–484, Mar. 1975.
[47] S. Das, I. Pan, S. Das, and A. Gupta, "Improved model reduction and tuning of fractional-order PIλDμ controllers for analytical rule extraction with genetic programming," *ISA Trans.*, vol. 51, no. 2, pp. 237–261, Mar. 2012.
[48] Q.-G. Wang, X. Guo, and Y. Zhang, "Direct identification of continuous time delay systems from step responses," *J. Process Control*, vol. 11, no. 5, pp. 531–542, Oct. 2001.
[49] M. A. Akbar, A. A. S. Ali, A. Amira, F. Bensaali, M. Benammar, M. Hassan, and A. Bermak, "An empirical study for PCA- and LDA-based feature reduction for gas identification," *IEEE Sensors J.*, vol. 16, no. 14, pp. 5734–5746, Jul. 2016.
[50] K. Ogata, *Modern Control Engineering*. Upper Saddle River, NJ, USA: Prentice-Hall, 2010.
[51] W. Wei, W. Xue, and D. Li, "On disturbance rejection in magnetic levitation," *Control Eng. Pract.*, vol. 82, pp. 24–35, Jan. 2019.
[52] Q.-L. Han and K. Gu, "On robust stability of time-delay systems with norm-bounded uncertainty," *IEEE Trans. Autom. Control*, vol. 46, no. 9, pp. 1426–1431, Sep. 2001.
[53] Y. Nesterov and A. Nemirovskii, *Interior-Point Polynomial Methods in Convex Programming*. Philadelphia, PA, USA: SIAM, 1994.
[54] P. Gahinet, A. Nemirovski, A. Laub, and M. Chilali, *LMI Control Toolbox*. Portola Valley, CA, USA: MathWorks, 1995.
[55] Y. Labit, D. Peaucelle, and D. Henrion, "SEDUMI INTERFACE 1.02: A tool for solving LMI problems with SEDUMI," in *Proc. IEEE Int. Symp. Comput. Aided Control Syst. Design*, Sep. 2002, pp. 272–277.
[56] I. R. Petersen, "A stabilization algorithm for a class of uncertain linear systems," *Syst. Control Lett.*, vol. 8, no. 4, pp. 351–357, Mar. 1987.
[57] P. Gahinet and P. Apkarian, "A linear matrix inequality approach to H_∞ control," *Int. J. Robust Nonlinear Control*, vol. 4, no. 4, pp. 421–448, 1994.
[58] K. Sundaravadivu, S. Sivakumar, and N. Hariprasad, "2DOF PID controller design for a class of FOPTD models—An analysis with heuristic algorithms," *Procedia Comput. Sci.*, vol. 48, pp. 90–95, Jan. 2015.
[59] S. Srivastava, A. Misra, S. K. Thakur, and V. S. Pandit, "An optimal PID controller via LQR for standard second order plus time delay systems," *ISA Trans.*, vol. 60, pp. 244–253, Jan. 2016.
[60] R. Sanz, P. Garcia, Q.-C. Zhong, and P. Albertos, "Predictor-based control of a class of time-delay systems and its application to quadrotors," *IEEE Trans. Ind. Electron.*, vol. 64, no. 1, pp. 459–469, Jan. 2017.
[61] S. Srivastava and V. S. Pandit, "A 2-DoF LQR based PID controller for integrating processes considering robustness/performance tradeoff," *ISA Trans.*, vol. 71, pp. 426–439, Nov. 2017.

VICENTE BALAGUER was born in Valencia, Spain, in 1993. He received the B.S. degree in industrial engineering and the M.S. degree in industrial engineering, with a focus on process control from the School of Industrial Engineering, Universitat Politècnica de València (UPV), in 2015 and 2017, respectively, where he is currently pursuing the Ph.D. degree. He has been a Visiting Researcher with Université de Technologie de Compiègne. His current research interests include control of unstable systems under the effect of disturbances, time-delay systems, and fault-tolerant control.

ANTONIO GONZÁLEZ received the degree (Hons.) in telecommunications engineering and the Ph.D. degree in automation and industrial informatics from the Universitat Politècnica de València (UPV), Spain, in 2012. He was a Postdoctoral Researcher with the Laboratory of Industrial and Human Automation control, Mechanical Engineering and Computer Science, CNRS, UMR 8201, Valenciennes, France, from 2013 to 2014. He currently works as an Associate Professor with the Department of Systems Engineering and Automation, Universitat Politècnica de València. His research interests include the broad area of time delay systems, robust control, networked control systems, multirobot systems, and process control applications.

PEDRO GARCÍA received the Ph.D. degree in computer science from the Universitat Politecnica de Valencia, Spain, in 2007. He has been a Visiting Researcher with the Lund Institute of Technology, Lund, Sweden; the Université de Technologie de Compiègne, France; the University of Florianopolis, Brazil; the University of Sheffield, U.K.; and the University of Zhejiang, Hangzhou, China. He is currently an Associate Professor with the Department of Systems Engineering and Automation, Universitat Politècnica de València. He has coauthored one book, and more than 90 refereed journal articles and conference papers. His current research interests include control of time-delay systems, disturbance observers, and control in type 1 diabetes.

FRANCISCO BLANES received the Ph.D. degree in computing sciences from the Universitat Politècnica de València (UPV).

From 2012 to 2020, he was the Director of the Instituto de Automática e Informática Industrial, (UPV), where he is currently teaching distributed and embedded real time systems. He has more than 90 scientific publications. His research interests include real-time embedded systems applied to robot control and distributed industrial control systems. During the last ten years, he has combined his research and teaching activities with innovation and collaboration with companies, and is responsible for many technology transfer projects in the area of smart manufacturing.